

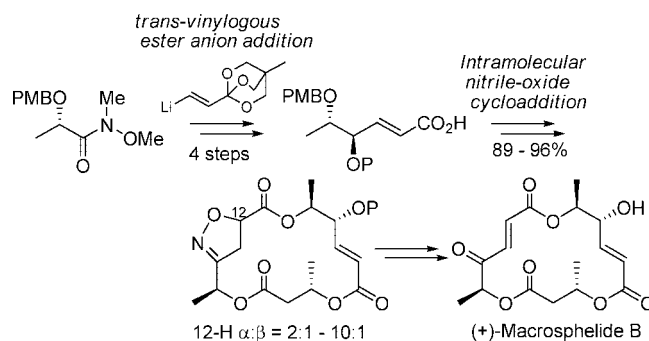
Concise Syntheses of (+)-Macrosphelides A and B: Studies on the Macro-Ring Closure Strategy

Seung-Mann Paek,[†] Hwayoung Yun,[†] Nam-Jung Kim,[†] Jong-Wha Jung,[†] Dong-Jo Chang,[†] Sujin Lee,[†] Jakyung Yoo,[‡] Hyun-Ju Park,[‡] and Young-Ger Suh*^{†,‡}

College of Pharmacy, Seoul National University, Gwanak-ro 599, Gwanak-gu, Seoul 151-742, Korea, and College of Pharmacy, Sungkyunkwan University, Suwon 440-746, South Korea

ygsuh@snu.ac.kr

Received August 9, 2008



Highly concise syntheses of (+)-macrosphelides A and B were accomplished in this study. The key feature of our synthetic route involved the direct three-carbon homologation of the readily available Weinreb amide **6** by the addition of a *trans*-vinylogous ester anion equivalent and facile construction of the 16-membered macrolide skeleton of macrosphelides via an intramolecular nitrile oxide–olefin cycloaddition. The syntheses of macrosphelides A and B were completed with a 30 and 20% overall yield, respectively. This paper describes the details of our syntheses.

Introduction

Naturally occurring macrolides continuously have been the focus of potential sources of drug leads because of their unique biological activities and structural features.¹ However, the enthalpic and entropic disadvantage of the macrocyclization process has hampered the development of efficient synthetic routes of biologically attractive natural macrolides and their analogs. A variety of macrocyclization technologies such as macrolactonization, ring-closing metathesis, and Pd(0)-catalyzed cross-coupling have been studied,² and these have been applied to the syntheses of synthetically and biologically attractive macrolides.³ However, the need for an efficient macrocyclization process, which retains versatility and selectivity, still exists.

From the first isolation⁴ and structural elucidation⁵ of macrosphelides from a culture broth of the fungus *Microsphaeropsis* sp. FO-5050 by the Omura group^{4a} and from the strain *Periconia byssoides* separated from the sea hare *Aplysia kurodai* by the Numata group,^{4c} these marine polyketides have attracted much interest from biologists because of their potent biological activities.^{4,5} (+)-Macrosphelide A selectively prohibits the adhesion of human leukemia HL-60 cells to human umbilical vein endothelial cells (HUVEC) in a dose-dependent fashion (IC₅₀ 3.5 μ M).^{4a} (+)-Macrosphelide A also exhibits oral

[†] Seoul National University.

[‡] Sungkyunkwan University.

(1) Dewick, P. M. *Medicinal Natural Products*, 2nd ed.; Wiley and Sons: Sussex, U.K., 2001.

(2) Parenty, A.; Moreau, X.; Campagne, J.-M. *Chem. Rev.* **2006**, *106* (3), 911–939.

(3) Kang, E. J.; Lee, E. *Chem. Rev.* **2005**, *105* (12), 4348–4378.

(4) (a) Hayashi, M.; Kim, Y.-P.; Hiraoka, H.; Natori, M.; Takamatsu, S.; Kawakubo, T.; Masuma, R.; Komiyama, K.; Omura, S. *J. Antibiot.* **1995**, *48*, 1435–1439. (b) Takamatsu, S.; Kim, Y.-P.; Hayashi, M.; Iraoka, H.; Natori, M.; Komiyama, K.; Omura, S. *J. Antibiot.* **1996**, *49*, 95–98. (c) Numata, A.; Iritani, M.; Yamada, T.; Minoura, K.; Matsumura, E.; Yamori, T.; Tsuruo, T. *Tetrahedron Lett.* **1997**, *38*, 8215–8218. (d) Yamada, T.; Iritani, M.; Doi, M.; Minoura, K.; Ito, T.; Numata, A. *J. Chem. Soc., Perkin Trans. 1* **2001**, 3046–3053. (e) Yamada, T.; Iritani, M.; Minoura, K.; Numata, A.; Kobayashi, Y.; Wang, Y.-G. *J. Antibiot.* **2002**, *55*, 147–154.

(5) (a) Sunazuka, T.; Hirose, T.; Harigaya, Y.; Takamatsu, S.; Hayashi, M.; Komiyama, K.; Omura, S.; Sprengeler, P. A.; Smith, A. B., III *J. Am. Chem. Soc.* **1997**, *119*, 10247–10248. (b) Sunazuka, T.; Hirose, T.; Chikaraishi, N.; Harigaya, Y.; Hayashi, M.; Komiyama, K.; Sprengeler, P. A.; Smith, A. B., III; Omura, S. *Tetrahedron* **2005**, *61* (15), 3789–3803.

antitumor activity against lung metastasis of B16/BL6 melanoma in mice (50 mg/kg).⁵ Importantly, no acute toxicity was produced by the injection of macrosphelide A into BDF mice intraperitoneally at 200 mg/kg for 5 days (Figure 1).⁴ In addition to anticancer activity, it also has been reported that the immunosuppressant activity of (+)-macrosphelide B is equally potent to that of cyclosporin, which is currently used clinically.⁶ Because of their anticancer and immunosuppressant properties, macrosphelides have been identified as a new lead target for the development of novel anticancer drugs and immunomodulators.⁷

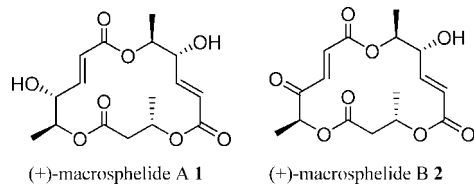


FIGURE 1. Structures of (+)-macrosphelides A and B.

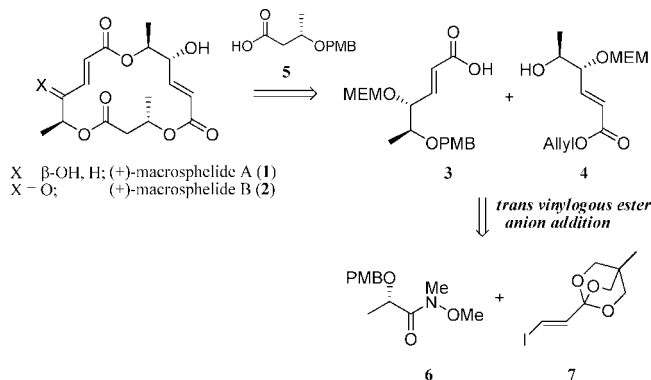
From a chemical perspective, macrosphelides are attractive because of their unique structural features.^{8–12} Macrosphelides consist of a 16-membered macrolide skeleton with three ester linkages connecting three fragments. Two of these fragments possess similar carbon frameworks and oxidation states. These unique structural features have prompted synthetic chemists to focus on the development of efficient synthetic methodologies for each fragment and for the macrocyclic ring closure. Previously, we reported the formal synthesis of (+)-macrosphelide A and the total synthesis of (+)-macrosphelide B. The methodology that was reported employed an efficient synthesis of the monomeric fragment by the direct addition of a *trans*-vinylogous ester anion equivalent to the corresponding carbonyl unit and an uncommon intramolecular nitrile oxide–olefin cycloaddition for the final macrolactonization reaction.¹³ This process appears to be superior to Yamaguchi lactonization^{8d,14} for labile cyclization precursors. The present report fully describes our synthetic efforts toward the syntheses of (+)-macrosphelides A and B.

Results and Discussion

Retrosynthesis toward 1. Our synthetic plan toward **1** is summarized in Scheme 1. First, we designed a unified strategy toward (+)-macrosphelides A (**1**) and B (**2**) because of their structural similarity. Therefore, we pursued the late-stage differentiation. From this point of view, our strategy envisaged a synthetic efficiency, including assembling key fragments **3**, **4**, and **5** through iterative esterification, followed by final macrolactonization. Key monomeric fragments **3** and **4** would be prepared conveniently through three-carbon homologation by addition of the *trans*-vinylogous acyl anion precursor **7**, which was developed by our group,¹⁵ to the

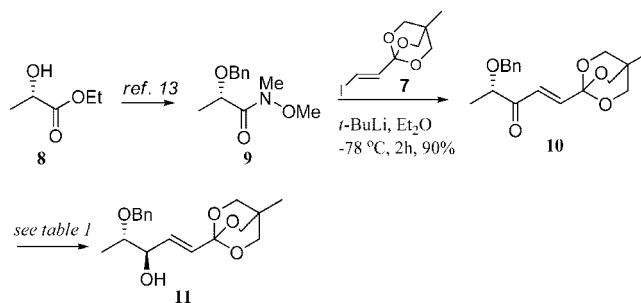
readily available Weinreb amide **6**. Employing this strategy, concise synthesis of **2** via sequential MEM deprotection and oxidation of the bis-protected acid **3** at the adequate stage was anticipated.

SCHEME 1. Retrosynthesis of (+)-Macrosphelide A



Our initial approach involved the addition of the *trans*-vinylogous acyl anion, prepared from **7**, to the corresponding Weinreb amide and the chelation-controlled reduction of the resulting ketone. Thus, we commenced our syntheses with the model study of the known Weinreb amide **9**¹⁶ (Scheme 2). Commercially available ethyl-(*S*)-lactate **8** was transformed into Weinreb amide **9**, which was subjected to the key three-carbon homologation. Gratifyingly, the addition of the vinyl anion prepared from **7**¹⁵ to the solution of **9** in Et₂O afforded the desired product **10** with a 90% yield. This one-step procedure afforded the entire carbon architecture of the key monomeric fragment **3**. After examination of the representative reduction conditions^{17–19} for the stereoselective ketone reduction of **10** with the latent ortho ester intact, the chelation-controlled 1,2-*anti* reduction was adapted for the requisite allylic alcohol **11**.

SCHEME 2. Vinylogous Ester Anion Addition to a Weinreb Amide



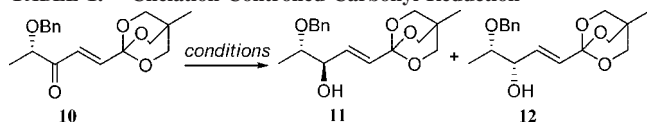
Initial reduction under Overman's condition¹⁷ (LAH, Et₂O, –10 °C) afforded poor selectivity (1.5:1). Addition of LiI¹⁸ as an additive elevated the diastereoselectivity slightly. However, super hydride reduction of **10** in CH₂Cl₂ enhanced the facial selectivity dramatically. This excellent facial selectivity is supported by Faucher's report.¹⁹

Lactic acid **13**²⁰ with the selectively cleavable PMB protecting group was transformed into Weinreb amide **6**. Subjection of **6** to the *trans*-vinylogous ester anion addition afforded the addition product **14** with a high yield. The diastereoselective reduction of **14** under the established conditions from the model study provided the 1,2-*anti* allylic alcohol **15** as a single detectable diastereomer. Finally, hydrolysis of the ortho ester after MEM

(6) Ōmura, S.; Komiyama, K. *Immunosuppressants*. PCT Int. Appl. WO 0147516 A1, 2001.

(7) For recent examples of medicinal research on macrosphelides, see: (a) Ishihara, K.; Kawaguchi, T.; Matsuya, Y.; Sakurai, H.; Saiki, I.; Nemoto, H. *Eur. J. Org. Chem.* **2004**, 3973–3978. (b) Matsuya, Y.; Kawaguchi, T.; Nemoto, H.; Nozaki, H.; Hamada, H. *Heterocycles* **2003**, *59*, 481–484. (c) Matsuya, Y.; Kawaguchi, T.; Nemoto, H. *Heterocycles* **2003**, *61*, 39–43. (d) Matsuya, Y.; Ishihara, K.; Funamori, N.; Kawaguchi, T.; Nemoto, H. *Heterocycles* **2003**, *61*, 59–63. (e) Matsuya, Y.; Nemoto, H. *Heterocycles* **2005**, *65*, 1741–1749. (f) Matsuya, Y.; Kawaguchi, T.; Ishihara, K.; Ahmed, K.; Zhao, Q.-L.; Kondo, T.; Nemoto, H. *Org. Lett.* **2006**, *8*, 4609–4612. (g) Wang, B.-L.; Jiang, Z.-X.; You, Z.-W.; Qing, F.-L. *Tetrahedron* **2007**, *63*, 12671–12680.

TABLE 1. Chelation-Controlled Carbonyl Reduction

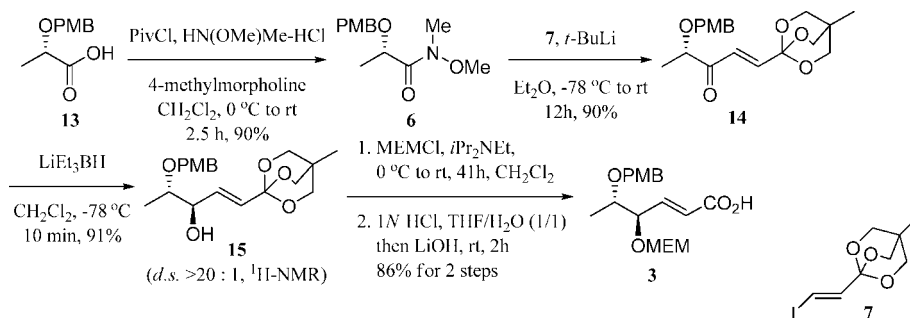


entry	reagent	solvent	yield (%)	ratio (11:12) ^a
1	LAH	Et ₂ O	79	1.5:1
2	LAH, Lil	Et ₂ O	80	3:1
3	LiEt ₃ BH	CH ₂ Cl ₂	80	>20:1

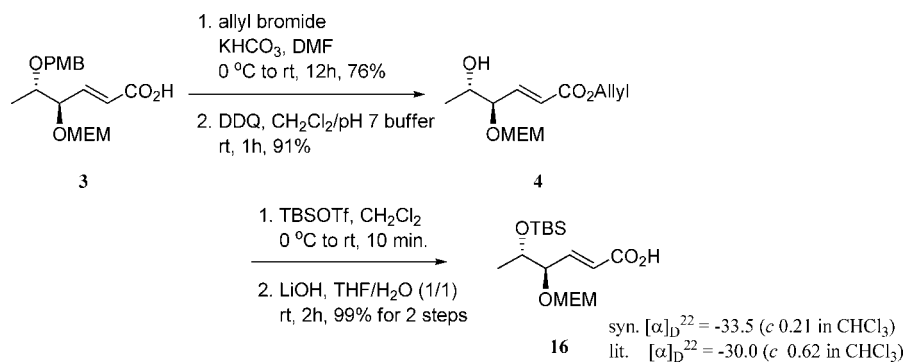
^a Diastereomeric ratio was determined by ¹H NMR.

protection of the secondary alcohol afforded the bis-protected acid **3**. This five-step sequence allowed us to secure a multigram quantity of the common fragment **3**, which was utilized for the total syntheses of both (+)-macrosphelides A and B.

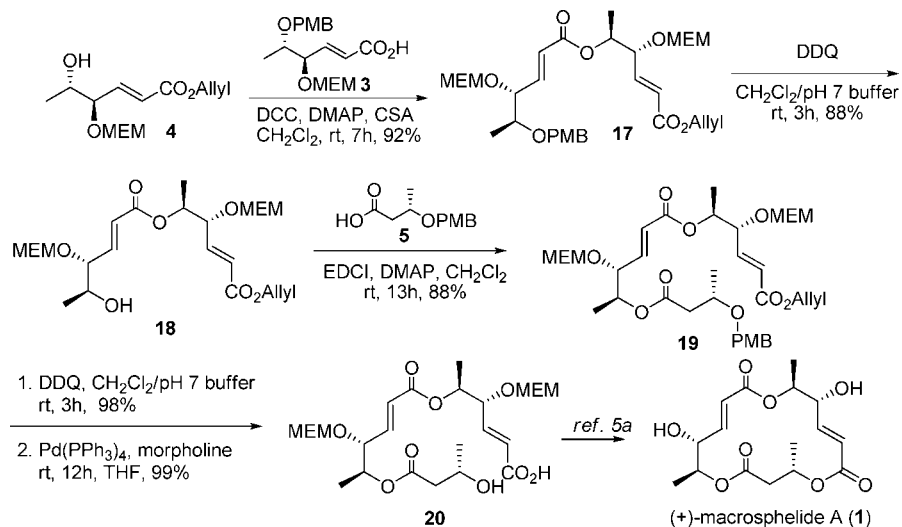
SCHEME 3. Preparation of Key Fragment 3



SCHEME 4. Structural Confirmation of Fragment 3



SCHEME 5. Formal Synthesis of (+)-Macrosphelide A



The structure of monomeric fragment **3** was confirmed as outlined in Scheme 4. Esterification of **3** with allyl bromide and oxidative cleavage of the PMB ether afforded homoallylic alcohol **4** with a 74% yield over two steps. Alcohol protection of **4**, followed by allyl deprotection, gave known acid **16**⁵ in a quantitative yield. The 1,2-*anti* diol **16** was identical to the reported **16** in all aspects, including optical rotation. This confirmation prompted us to complete the synthesis of **1** by the coupling of **3** with intermediate **4** (Scheme 5).

Synthesis of **1** commenced with the coupling of fragments **3** and **4** (Scheme 5). Acid **3** and homoallylic alcohol **4** were coupled by esterification under Keck conditions,²¹ and the PMB ether was deprotected by DDQ to produce alcohol **18**. Again, esterification of acid **5**²² and alcohol **18** afforded trimeric ester **19** with a yield of 88%. Finally, PMB deprotection of **19**,

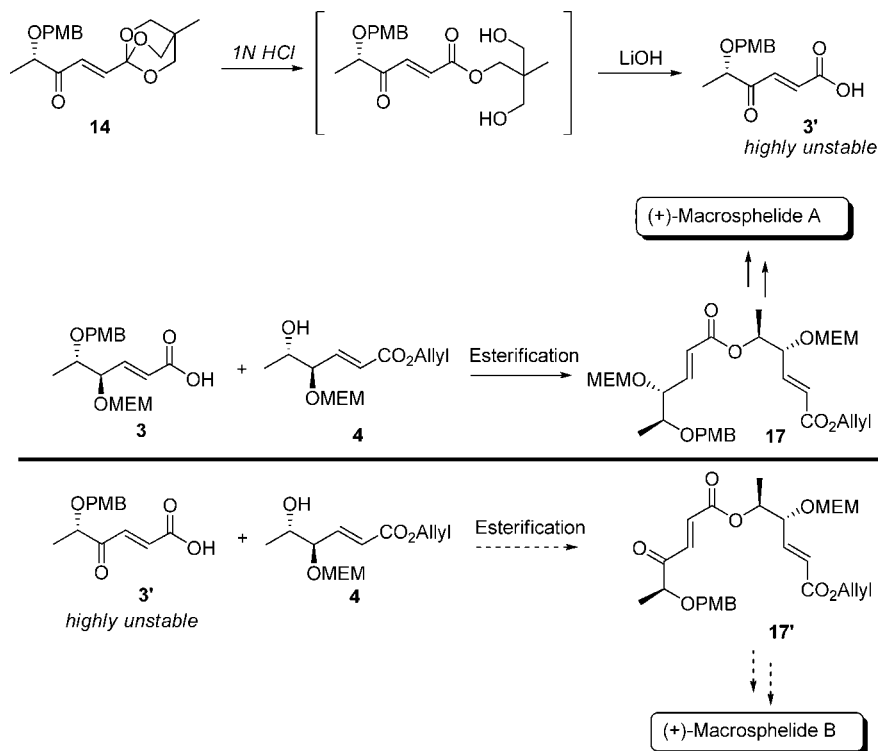


FIGURE 2. First synthetic plan for (+)-macrosphelide B.

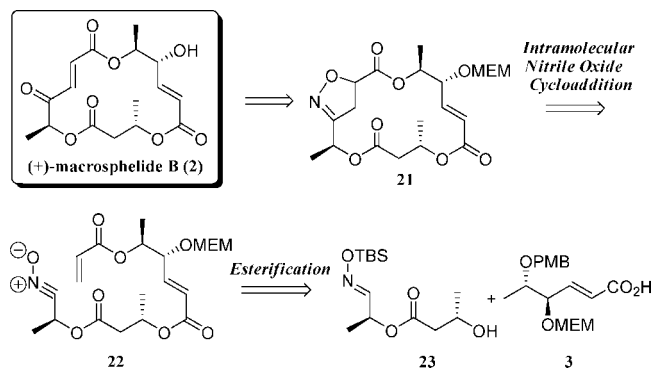
followed by allyl ester cleavage in the presence of $\text{Pd}(\text{PPh}_3)_4$, afforded the known seco acid **20** in a near quantitative yield. The structure of seco acid **20** was confirmed by comparison of its spectral data with that reported for compound **20**.⁵

Synthetic Study toward 2. After completion of the formal synthesis of **1**, we turned our attention toward the total synthesis of **2** (Figure 2). The structural similarity of **1** and **2** envisioned the utilization of fragment **3'** as a coupling partner for the synthesis of **2**, using the same strategy employed for the synthesis of macrosphelide A. However, the highly electron-deficient character as well as the free acid function of **3'** hampered this approach.²³ Thus, an alternative route employing a masked variant of the reactive γ -keto- α,β -unsaturated carbonyl moiety was necessary.

Revised Retrosynthesis toward 2. Because the instability of the α,β -unsaturated γ -keto acid moiety rendered our initial iterative approach toward **2** unsuccessful, we decided to expose it at the late stage of our synthesis. Therefore, we chose an isoxazoline unit as a suitable equivalent in terms of stability and facile conversion to **2** (Scheme 6). The isoxazoline intermediate **21** envisaged an efficient synthesis of (+)-macrosphelide **2** upon facile N–O bond cleavage²⁴ of **21** and subsequent dehydration of the secondary alcohol at the final stage. For isoxazoline **21**, we planned to employ an intramolecular nitrile oxide–olefin cycloaddition (INOC) because the previous macrocyclic INOC executed by Asaoka and Kim²⁵ provided the desired regioselectivity. The INOC enabled the introduction of the masked γ -keto- α,β -unsaturated acid moiety at the late stage and also constructed the core 16-membered lactone skeleton of macrosphelide as the final ring closure

instead of Yamaguchi lactonization, which is known to induce a partial racemization.^{8d} Nitrile oxide **22** would readily be prepared in situ from the intermediate obtained by esterification of oxime ether **23** and key fragment **3**.

SCHEME 6. Revised Synthetic Strategy for (+)-Macrosphelide B



Preparation of INOC Precursor 29. Preparation of INOC precursor **29** is described in Scheme 7. Known aldehyde **24**²⁶ was condensed with commercially available TBS-protected hydroxylamine to give oxime ether **25**. Although separation of the *E/Z* mixture of **25** was possible by careful column chromatography on silica gel, it was directly used for the next step because both isomers could be transformed into nitrile oxide **22**. PMB deprotection of **25** and esterification of the resulting alcohol with acid **5** followed by PMB removal of the resulting ester **26** afforded a 59% yield of alcohol **23** in three steps. Alcohol **23** was coupled with key fragment **3** under Yamaguchi conditions to afford diester **27** with a 74% yield.²⁷ Oxidative cleavage of the PMB ether of **27** and subsequent acryloylation of the resulting alcohol gave TBS oxime **28**. Deprotection of

(8) (a) Kobayashi, Y.; Kumar, B. G.; Kurachi, T. *Tetrahedron Lett.* **2000**, *41*, 1559–1563. (b) Kobayashi, Y.; Kumar, G. B.; Kurachi, T.; Acharya, H. P.; Yamazaki, T.; Kitazume, T. *J. Org. Chem.* **2001**, *66*, 2011–2018. (c) Kobayashi, Y.; Acharya, H. P. *Tetrahedron Lett.* **2001**, *42*, 2817–2820. (d) Kobayashi, Y.; Wang, Y.-G. *Tetrahedron Lett.* **2002**, *43*, 4381–4384.

SCHEME 7. Preparation of INOC Precursor 29

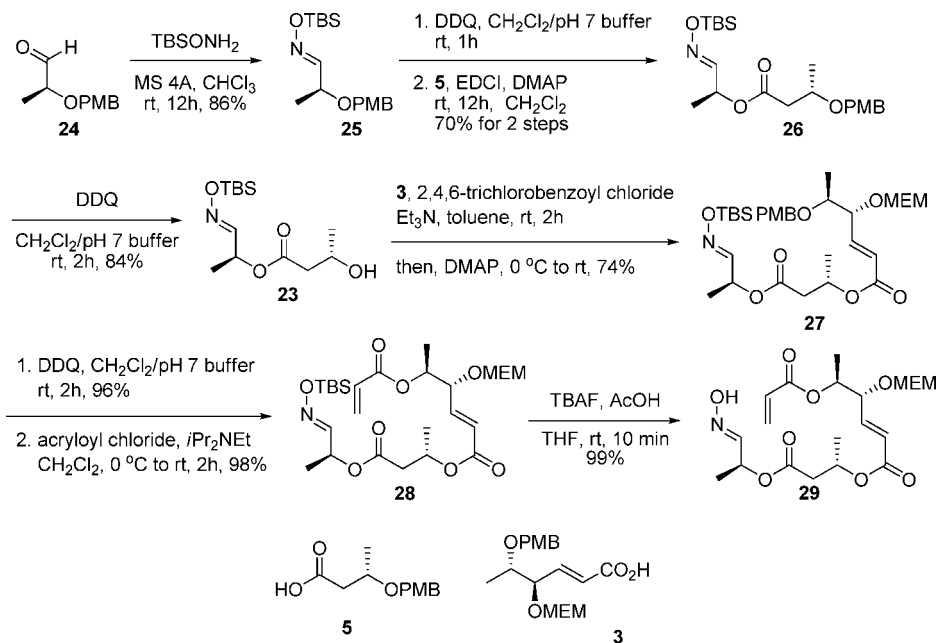
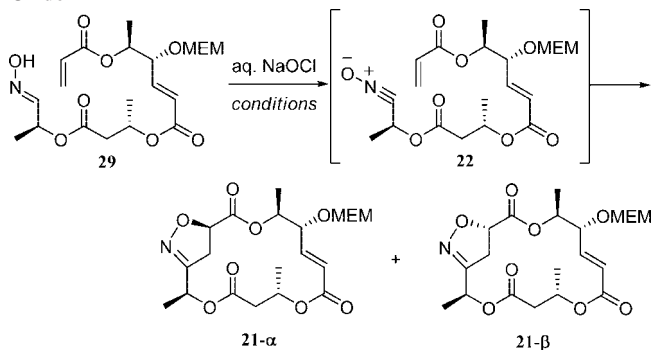


TABLE 2. Intramolecular Cycloaddition of Olefin and Nitrile Oxide



entry	solvent	temperature (°C)	ratio (21-α:21-β)	yield (%)
1	CH ₂ Cl ₂	rt	66:33	96
2	CH ₂ Cl ₂	-78	no reaction	—
3	CH ₂ Cl ₂	-30	83:17	50
4	CH ₂ Cl ₂	-15	83:17	79
5	CH ₂ Cl ₂	40	54:46	37
6	THF	-15	88:12	47
7	benzene	-15	93:17	22
8	1,4-dioxane	rt	91:9	89

oxime **28** under the buffered TBAF conditions provided requisite free oxime **29** with the other labile functional groups intact in a near quantitative yield.

Intramolecular Nitrile Oxide Cycloaddition (INOC). With the desired free oxime **29** available, we investigated a variety of conditions to produce the desired INOC adduct (Table 2). Gratifyingly, use of NaOCl as an oxidant in CH₂Cl₂ at room temperature afforded the INOC adducts as a mixture of **21-α** and **21-β** with a 96% yield and without detection of the undesired regioisomers. The facial selectivity was moderate (2:1), and both diastereomers were separated by column chromatography (Table 2, entry 1). Considering the ultimate disappearance of the newly formed stereogenic center in our synthesis, the moderate facial selectivity seems unimportant. However, we improved the diastereoselectivity of the INOC because we discovered that minor adduct **21-β** was a poor

substrate in the N–O bond cleavage, which lowered the overall efficiency of our synthesis (Scheme 8). The low reaction temperature improved the facial selectivity, although the chemical yield was not satisfactory (Table 2, entries 2–4). Cycloaddition under reflux conditions did not work (Table 2, entry 5). However, cycloaddition in 1,4-dioxane instead of THF (Table 2, entry 6) or benzene (Table 2, entry 7) afforded a high facial selectivity as well as an excellent yield.

Structural assignments of the INOC adducts, **21-α** and **21-β**, are outlined in Scheme 9. Major adduct **21-α** was treated with a catalytic amount of NaH in MeOH to give the methanolysis product **30**. The free hydroxyl group of **30** was removed by tosylation and subsequent super hydride treatment, which also reduced the methyl ester to give the primary alcohol **32**. The optical rotation of isoxazoline **32** was identical to that of authentic **32**,²⁸ and this confirmed the absolute stereochemistry of 12-C of major adduct **21-α**. Stereochemical elucidation of the new stereocenter seems interesting in terms of understanding the INOC pattern for the macrocyclic ring closure of this unique system. Furthermore, from the viewpoint of medicinal chemistry, a variety of structural variants of macrosphelides could be derived from these INOC intermediates.

The plausible transition state of INOC for oxime **29** is illustrated in Figure 3. Exposure of oxime **29** to NaOCl produces the nitrile oxide **22** in situ, which undergoes [3 + 2] intramolecular nitrile oxide–olefin cycloaddition to pro-

(9) (a) Ono, M.; Nakamura, H.; Konno, F.; Akita, H. *Tetrahedron: Asymmetry* **2000**, *11*, 2753–2764. (b) Nakamura, H.; Ono, M.; Shiba, Y.; Akita, H. *Tetrahedron: Asymmetry* **2002**, *13*, 705–713. (c) Nakamura, H.; Ono, M.; Makino, M.; Akita, H. *Heterocycles* **2002**, *57*, 327–336.

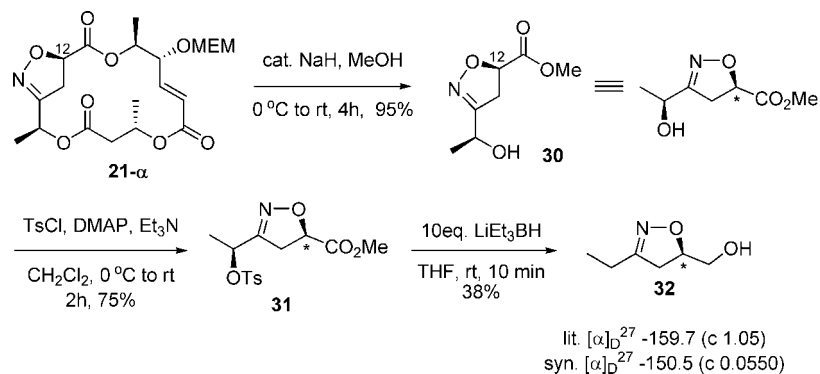
(10) Sharma, G. V. M.; Mouli, C. C. *Tetrahedron Lett.* **2002**, *43*, 9159–9161.

(11) (a) Takahashi, T.; Kusaka, S.-i.; Doi, T.; Sunazuka, T.; Omura, S. *Angew. Chem., Int. Ed.* **2003**, *42*, 5230–5234. (b) Kusaka, S.-I.; Dohi, S.; Doi, T.; Takahashi, T. *Tetrahedron Lett.* **2003**, *44*, 8857–8859.

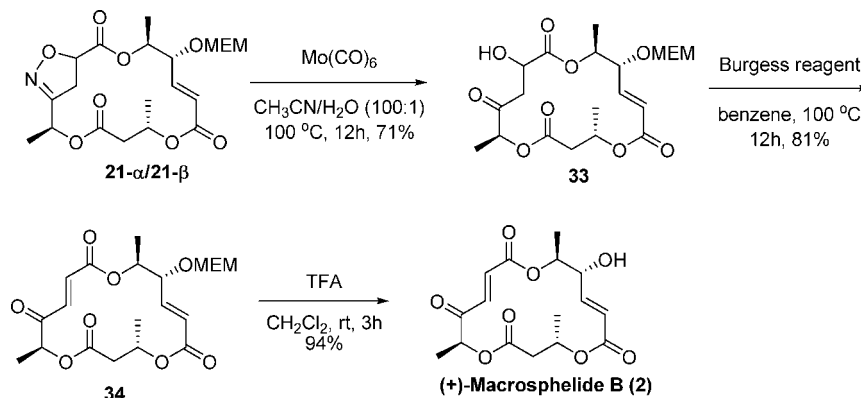
(12) (a) Matsuya, Y.; Kawaguchi, T.; Nemoto, H. *Org. Lett.* **2003**, *5*, 2939–2941. (b) Kawaguchi, T.; Funamori, N.; Matsuya, Y.; Nemoto, H. *J. Org. Chem.* **2004**, *69*, 505–509.

(13) Paek, S.-M.; Seo, S.-Y.; Kim, S.-H.; Jung, J.-W.; Lee, Y.-S.; Jung, J.-K.; Suh, Y.-G. *Org. Lett.* **2005**, *7*, 3159–3162.

(14) Inanaga, J.; Hirata, K.; Saeki, H.; Katsuki, T.; Yamaguchi, M. *Bull. Chem. Soc. Jpn.* **1979**, *52*, 1989–1993.

SCHEME 8. Structural Confirmation of INOC Major Adduct 21- α 

SCHEME 9. Completion of (+)-Macrosphelide B Synthesis



duce isoxazoline intermediates **21- α** and **21- β** . During the cycloaddition of nitrile oxide and olefin, the α -face approach of the acrylate moiety of **22** toward the nitrile oxide seems to suffer a steric interaction between the two vinyl hydrogens of the acrylate and the 15-H of the nitrile oxide. In contrast, the β -face approach of the acrylate moiety creates a severe

steric repulsion of the vinyl hydrogens of the acrylate and 15-CH₃ group of the nitrile oxide. This difference in the steric repulsion of the two transition states seems to induce production of **21- α** as a favorable adduct, and this facial selectivity is consistent with the previous report by Shishido.²⁹

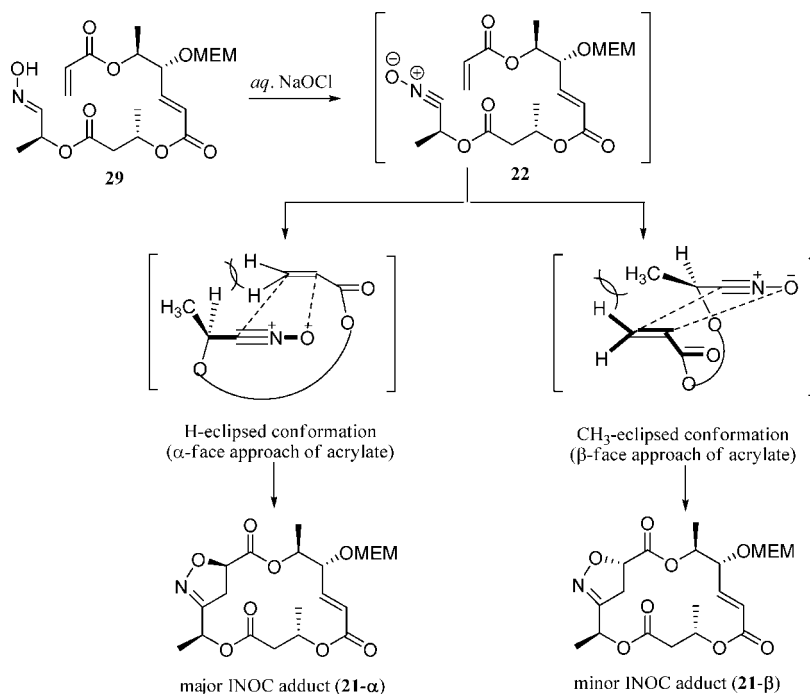


FIGURE 3. Transition state for INOC.

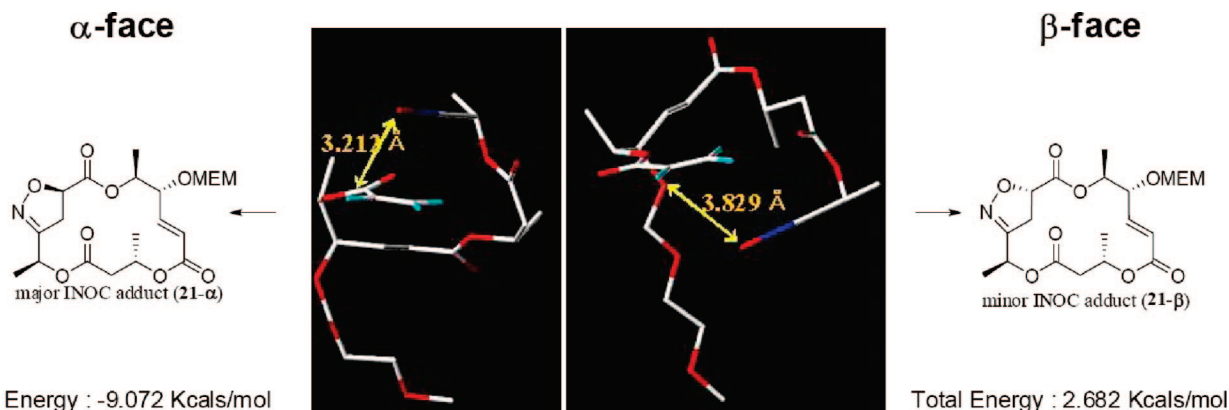


FIGURE 4. Energy-minimized transition states for INOC.

Further analysis of our proposed mechanism is in Figure 3. Molecular modeling was conducted to generate transition state geometries in the INOC. A conformational search of transition state **22**, performed by molecular dynamics using a simulated annealing method, provided a conformer library containing more than 500 conformations. From the conformer library of **22**, the structures that mimic the transition state for the attack from α face and β face in the INOC were selected. The selected structures were energy minimized, and these structures are in Figure 4. As we anticipated, the transition state for the attack from the α face was energetically more favorable than that from the β face, when comparing energies and the distances between the oxygen atom of the nitrile oxide and the vinyl carbon of the acrylate moiety. These results support the experimental results obtained with INOC, in which isomer **21- α** was obtained as the major product.

Completion of Synthesis toward **2.** The mixture of INOC adduct **21- α** and **21- β** was treated with $\text{Mo}(\text{CO})_6$ in wet CH_3CN to give the secondary alcohol **33** (Scheme 9). Spectral analysis (^{13}C NMR) confirmed the structure of **33**, which consists of a single diastereomer. Production of a single diastereomer is likely due to the favorable reaction profile for **21- α** compared to that for **21- β** .³⁰ Dehydration of alcohol **33** afforded a known MEM-protected (+)-macrosphelide **B** **34** with a yield of 81%, and the final MEM deprotection of **34**¹² provided **2** in an excellent yield. This synthetic (+)-macrosphelide **B** (**2**) exhibited spectral data (^1H NMR, ^{13}C NMR, HR-MS, IR) and optical rotation identical to those of the authentic natural product.

Conclusion

In summary, we achieved the formal synthesis of (+)-macrosphelide **A** through 12 linear steps with a 30% overall

yield and the total synthesis of (+)-macrosphelide **B** through 13 linear steps with a 20% overall yield. The synthetic approach used the efficient preparation of key fragments and the highly convergent assembly of these fragments, including the 16-membered ring formation by INOC from the highly labile precursors. The key architecture of the monomeric fragment involves the direct addition of the *trans*-vinylogous ester anion to the corresponding Weinreb amide, followed by a chelation-controlled stereoselective carbonyl reduction. In particular, the INOC-induced ring closure for the synthesis of (+)-macrosphelide **B** would be highly suitable for the versatile and practical syntheses of macrosphelide analogs. Employing this practical synthetic route, our intensive work on the macrosphelide analogs with promising pharmacological properties is currently in progress.

Experimental Section

Addition of the Vinylogous Ester Anion. (*S,E*)-4-(4-Methoxybenzyloxy)-1-(4-methyl-2,6,7-trioxabicyclo[2.2.2]octan-1-yl)pent-1-en-3-one **14**: To a solution of *t*-BuLi (1.5 M solution in pentane, 3.8 mL, 5.7 mmol) in Et_2O (10 mL) at -78°C was added a solution of iodovinyl ortho ester **7** (810 mg, 2.9 mmol) in Et_2O (10 mL). After the mixture was stirred for 5 h at -40°C , a solution of Weinreb amide **6** (170 mg, 0.70 mmol) in Et_2O (10 mL) was added at -78°C . The reaction mixture was warmed to rt and stirred for 12 h, after which it was quenched with H_2O . The reaction mixture was extracted with EtOAc , and the combined organic layers were washed with brine, dried over Na_2SO_4 , and concentrated in vacuo. The residue was purified by flash column chromatography on silica gel (EtOAc/n -hexane/ Et_3N , 25:75:2) to afford 220 mg (90%) of ketone **14** as a colorless oil: $[\alpha]_D^{20} -3.75$ (*c* 0.5, MeOH); ^1H NMR (CD_3OD , 300 MHz) δ 7.19 (d, 2H, $J = 8.8$ Hz), 6.82 (d, 2H, $J = 8.8$ Hz), 6.75 (d, 1H, $J = 15.7$ Hz), 6.51 (d, 1H, $J = 15.9$ Hz),

(23) Although Y. Kobayashi reported the synthesis of **3'**, we couldn't handle that compound. This difference is thought to be derived from the highly labile character of **3'**. See ref 8.

(24) Baraldi, P. G.; Barco, A.; Benetti, S.; Manfredini, S.; Simoni, D. *Synthesis* **1987**, 276–278.

(25) (a) Asaoka, M.; Abe, M.; Mukata, T.; Takei, H. *Chem. Lett.* **1982**, 11, 215–218. (b) Kim, D.; Lee, J.; Shim, P. J.; Doi, T.; Kim, S. *J. Org. Chem.* **2002**, 67, 772–781.

(26) Maezaki, N.; Hirose, Y.; Tanaka, T. *Org. Lett.* **2004**, 6, 2177–2180.

(27) Esterification under other various conditions such as EDCI-DMAP, DCC-DMAP, or DCC-DMAP-CSA was unsuccessful.

(28) Curran, D. P.; Kim, B. H.; Daugherty, J.; Heffner, T. A. *Tetrahedron Lett.* **1988**, 29, 3555–3558.

(29) Irie, O.; Fujiwara, Y.; Nemoto, H.; Shishido, K. *Tetrahedron Lett.* **1996**, 37, 9229–9232.

(30) When pure **21- β** was transformed to **34**, the two-step yield was 5–10%. This may be a result from the reluctance of **21- β** to bond with N–O cleavage.

4.33 (dd, 2H, $J = 10.9, 24.0$ Hz), 4.05 (q, 1H, $J = 7.0$ Hz), 3.91 (s, 6H), 3.71 (s, 3H), 1.21 (d, 3H, $J = 7.0$ Hz), 0.75 (s, 3H); ^{13}C NMR (CD_3OD , 125 MHz) δ 203.6, 161.6, 140.9, 131.6 (2C), 128.3, 115.5, 107.6, 81.3, 74.6, 73.3, 56.4, 32.2, 18.6, 15.0; IR (neat) ν_{max} 3744, 2877, 1701, 1649, 1512, 1461, 1324, 1247 cm^{-1} ; LRMS (FAB) m/z 349 ($\text{M} + \text{H}^+$); HRMS (FAB) calcd for $\text{C}_{19}\text{H}_{25}\text{O}_6$ ($\text{M} + \text{H}^+$) 349.1651, found 349.1657.

Intramolecular Nitrile Oxide Cycloaddition. (2*S*,6*S*,11*R*,12*S*,15*R*)-11-[(2-Methoxyethoxy)methoxy]-2,6,12-trimethyl-3,7,13,16-tetraoxa-17-azabicyclo[13.2.1]octadeca-1(17),9-diene-4,8,14-trione **21- α** and (2*S*,6*S*,11*R*,12*S*,15*S*)-11-[(2-methoxyethoxy)methoxy]-2,6,12-trimethyl-3,7,13,16-tetraoxa-17-azabicyclo[13.2.1]octadeca-1(17),9-diene-4,8,14-trione **21- β** : To a solution of aldoxime **29** (3.0 mg, 6.7 μmol) in dioxane (1 mL) was added aqueous NaOCl (about 10%, 5 drops) at ambient temperature. The reaction mixture was stirred for 10 min at the same temperature and diluted with H_2O . The aqueous layer was extracted with CH_2Cl_2 , and the combined organic layers were dried over MgSO_4 and concentrated in vacuo. The residue was purified by flash column chromatography on silica gel (EtOAc/*n*-hexane, 2:3 \rightarrow 3:2) to afford 2.5 mg (83%) of isoxazoline **21- α** and 0.2 mg (6.6%) of isoxazoline **21- β** as colorless oils. **21- α** : $[\alpha]_{\text{D}}^{20} -107.5$ (c 0.8, CHCl_3); ^1H NMR (CDCl_3 , 400 MHz) δ 6.68 (dd, 1H, $J = 4.7, 15.7$ Hz), 6.00 (d, 1H, $J = 15.7$ Hz), 5.47 (q, 1H, $J = 6.5$ Hz), 5.33–5.30 (m, 1H), 5.00 (dd, 1H, $J = 7.5, 11.7$ Hz), 4.89 (dq, 1H, $J = 4.0, 6.4$ Hz), 4.69 (dd, 2H, $J = 7.0, 13.2$ Hz), 4.21 (t, 1H, $J = 8.0$ Hz), 3.78–3.73 (m, 1H), 3.64–3.59 (m, 1H), 3.55–3.51 (m, 2H), 3.37 (s, 3H), 3.22 (dd, 1H, $J = 11.9, 17.6$ Hz), 3.07 (dd, 1H, $J = 7.5, 17.6$ Hz), 2.69–2.59 (m, 2H), 1.56 (d, 3H, $J = 6.6$ Hz), 1.42 (d, 3H, $J = 6.2$ Hz), 1.33 (d, 3H, $J = 6.3$ Hz); ^{13}C NMR (CDCl_3 , 100 MHz) δ 170.3, 169.1,

164.5, 157.4, 144.5, 125.1, 93.6, 78.1, 77.2, 77.1, 72.3, 71.5, 67.9, 67.4, 65.9, 59.0, 40.6, 40.4, 19.7, 17.4; IR (neat) ν_{max} 2924, 1739, 1455, 1371, 1272, 1187, 1051, 852 cm^{-1} ; LRMS (EI) m/z 443 ($\text{M} + \text{Na}^+$); HRMS (FAB) calcd for $\text{C}_{20}\text{H}_{30}\text{NO}_{10}$ ($\text{M} + \text{H}^+$) 444.1870, found 444.1881. **21- β** : $[\alpha]_{\text{D}}^{20} -55.1$ (c 1.16, CHCl_3); ^1H NMR (CDCl_3 , 300 MHz) δ 6.67 (dd, 1H, $J = 7.8, 15.9$ Hz), 5.99 (d, 1H, $J = 15.9$ Hz), 5.77 (q, 1H, $J = 6.9$ Hz), 5.45–5.39 (m, 1H), 4.95 (dd, 1H, $J = 8.4, 12.2$ Hz), 4.94 (dq, 1H, $J = 6.2, 9.3$ Hz), 4.74 (dd, 2H, $J = 7.1, 16.1$ Hz), 4.05 (t, 1H, $J = 8.7$ Hz), 3.78–3.72 (m, 1H), 3.65–3.58 (m, 1H), 3.53–3.50 (m, 2H), 3.38–3.26 (m, 1H), 3.36 (s, 3H), 2.82 (dd, 1H, $J = 8.2, 17.5$ Hz), 2.66–2.53 (m, 2H), 1.48 (d, 3H, $J = 6.7$ Hz), 1.36 (d, 3H, $J = 6.2$ Hz), 1.30 (d, 3H, $J = 6.3$ Hz); ^{13}C NMR (CDCl_3 , 125 MHz) δ 169.6, 167.8, 164.0, 158.3, 145.3, 125.3, 93.8, 77.6, 76.4, 71.5, 71.4, 68.1, 67.4, 66.5, 58.9, 40.9, 39.0, 19.9, 19.1, 17.6; IR (neat) ν_{max} 2925, 2854, 1742, 1455, 1374, 1252, 1192, 1104, 1051 cm^{-1} ; LRMS (FAB) m/z 444 ($\text{M} + \text{H}^+$); HRMS (FAB) calcd for $\text{C}_{20}\text{H}_{30}\text{NO}_{10}$ ($\text{M} + \text{H}^+$) 444.1870, found 444.1854.

Acknowledgment. This research was supported by the Center for Bioactive Molecular Hybrids, Yonsei University, and in part by the Research Institute of Pharmaceutical Science, Seoul National University.

Supporting Information Available: Experimental procedures and spectroscopic data. This material is available free of charge via the Internet at <http://pubs.acs.org>.

JO8016692